Modern Pathology (2009) 22, 1121–1131

www.modernpathology.org

Chromosomal instability, telomere shortening, and inactivation of p21$^{WAF1/CIP1}$ in dysplastic nodules of hepatitis B virus-associated multistep hepatocarcinogenesis

Yoon Hee Lee[1,2,*], Bong-Kyeong Oh[3,4,*], Jeong Eun Yoo[1], So-Mi Yoon[1], Jinsub Choi[5], Kyung Sik Kim[5] and Young Nyun Park[1]

[1]*Department of Pathology, Institute of Gastroenterology, Brain Korea 21 Project for Medical Science, Center for Chronic Metabolic Disease, Yonsei University College of Medicine, Seoul, Korea;* [2]*Department of Pathology, CHA Gangnam Medical Center, CHA University, Seoul, Korea;* [3]*Bio/Molecular Informatics Center, Konkuk University, Seoul, Korea;* [4]*Cancer Metastasis Research Center, Yonsei University College of Medicine, Seoul, Korea and* [5]*Department of Surgery, Yonsei University College of Medicine, Seoul, Korea*

Systemic analysis for chromosomal instability and inactivation of cell cycle checkpoints are scarce during hepatocarcinogenesis. We studied 24 patients with chronic B viral cirrhosis including 30 cirrhotic regenerative nodules, 35 low-grade dysplastic nodules, 15 high-grade dysplastic nodules, 7 dysplastic nodules with hepatocellular carcinoma foci, and 18 hepatocellular carcinomas. Eight normal livers were studied as the control group. Telomere length and micronuclei were detected by Southern blot and Feulgen-fast green dyeing technique, respectively, and p21$^{WAF1/CIP1}$ expression was studied by immunohistochemistry. Micronuclei >1 per 3000 hepatocytes were found in 17% of low-grade dysplastic nodules, 87% of high-grade dysplastic nodules, and 100% of high-grade dysplastic nodules with hepatocellular carcinoma foci and hepatocellular carcinomas in contrast to those of all normal livers, and 90% of cirrhosis showed no micronuclei. The micronuclei index showed a gradual increase during hepatocarcinogenesis and there was a significant increase between cirrhosis and low-grade dysplastic nodules, low-grade dysplastic nodules and high-grade dysplastic nodules, and high-grade dysplastic nodules and hepatocellular carcinomas. Telomere length showed a gradual shortening during hepatocarcinogenesis and a significant reduction was found in high-grade dysplastic nodules ($P=0.024$) and hepatocellular carcinomas ($P=0.031$) compared with normal and cirrhotic livers. The micronuclei index was correlated with telomere shortening ($P=0.016$). The p21$^{WAF1/CIP1}$ labeling index was significantly higher in cirrhosis than in normal livers ($P=0.024$) and markedly decreased in low-grade dysplastic nodules, high-grade dysplastic nodules, and hepatocellular carcinomas compared with cirrhosis ($P<0.05$). The p21$^{WAF1/CIP1}$ labeling index was associated with telomere length ($P<0.001$) but not micronuclei index. This study shows that telomere shortening, chromosomal instability, and inactivation of p21$^{WAF1/CIP1}$ checkpoint function occur in low-grade dysplastic nodules as well as in high-grade dysplastic nodules, and their cooperation is considered to be critical for malignant transformation during hepatitis B virus associated-multistep hepatocarcinogenesis.
Modern Pathology (2009) **22,** 1121–1131; doi:10.1038/modpathol.2009.76; published online 22 May 2009

Keywords: dysplastic nodule; hepatocellular carcinoma; chromosomal instability; p21$^{WAF1/CIP1}$; telomere; hepatitis B virus

Hepatocellular carcinoma is the fifth most common cancer and the prognosis of patients with hepatocellular carcinoma is generally very poor, therefore, the diagnosis and treatment of precancerous lesions in the early stage of hepatocarcinogenesis is important.[1] Dysplastic nodules, which usually occur in cirrhotic livers, are nodular lesions that differ from the surrounding parenchyma with regard to size, color, and texture. Dysplastic nodules can be classified as low or high grade according to the degree of cytological and architectural atypia on histological examination.[2] High-grade dysplastic nodules have been reported to have pathological

Correspondence: Professor YN Park, MD, PhD, Department of Pathology and Brain Korea 21 Project for Medical Science, Yonsei University College of Medicine, 134 Shinchon-dong, Seodaemoon-gu, Seoul 120-752, Korea.
E-mail: young0608@yuhs.ac
*These two authors contributed equally to this work.
Received 20 November 2008; revised 7 April 2009; accepted 16 April 2009; published online 22 May 2009

characteristics similar to hepatocellular carcinomas, but the nature of low-grade dysplastic nodules has not been clearly described.[3,4] Two recent follow-up studies reported the natural history of large hepatic nodules. Borzio *et al* followed 90 cirrhotic patients with histologically proven large regenerative nodules ($n=56$), low-grade dysplastic nodules ($n=16$), and high-grade dysplastic nodules ($n=19$), and reported that the presence of high-grade dysplastic nodules was associated with an increased hazard risk for hepatocellular carcinoma (2.4 over a mean follow-up period of 33 months). However, low-grade dysplastic nodules were not at increased risk for hepatocellular carcinoma development.[5] In another study, Kobayashi *et al* followed 154 patients with histologically proven large regenerative nodules ($n=99$), low-grade dysplastic nodules ($n=42$), and high-grade dysplastic nodules ($n=23$) for a median period of 2.8 years. The hazard ratios for high-grade dysplastic nodule, low-grade dysplastic nodule, and large regenerative nodule for hepatocellular carcinoma development were 16.8, 2.96, and 1, respectively, and approximate annual development rate to hepatocellular carcinoma was 20% in patients with high-grade dysplastic nodule and 10% in those with low-grade dysplastic nodule.[6]

The telomere is a TTAGGG-repeat sequence located at the end of the chromosome that is not replicated during the S phase of the cell cycle, and is shortened with each cell division of somatic cells.[7] When telomeres shorten to a critical length, cells lose their telomere-capping function and suffer genetic changes because of chromosomal instability, defined as an increased rate of chromosome aberrations and aneuploidies, particularly involving breakage/fusion/bridge cycles after telomere loss.[8] Most hepatocellular carcinomas are characterized by chromosomal instability with aneuploidy and chromosomal aberrations, which is more common in hepatitis B virus-associated hepatocellular carcinomas.[9–11] We earlier reported a gradual telomere shortening in the progression of human multistep hepatocarcinogenesis.[12,13] A significant telomere shortening occurred during the transition from low-grade dysplastic nodules to high-grade dysplastic nodules, and hepatocellular carcinomas showed the shortest telomere length. It is interesting to note that 14–17% of low-grade dysplastic nodules showed a shortening of telomere length up to the level of high-grade dysplastic nodules, and there was no histological difference between low-grade dysplastic nodules with or without telomere shortening.[12]

The micronucleus, an indicator of chromosome damage, arises from chromosome fragments or whole chromosomes in the anaphase and telophase stages and manifest as small nuclei in the cytoplasm of interphase cells, and therefore are regarded as indicators of genomic instability in dividing cells.[14–19] In rodent models of experimental hepatocarcinogenesis, the number of micronuclei increased with progression of hepatocarcinogenesis as measured by genetic alterations.[16,17] Micronucleated hepatocytes have also been reported to be significantly more frequent in hepatocellular carcinomas compared with cirrhotic regenerative nodules and normal hepatic parenchyma.[19] However, little is known about micronuclei formation in defined pathological lesions including dysplastic nodules of human multistep hepatocarcinogenesis.

The loss of telomere integrity induces a DNA damage response involving the cell cycle checkpoint pathways, which leads to permanent cell cycle arrest at the senescence stage.[7,20,21] Senescence is regarded as a tumor suppressor mechanism that prevents proliferation of genetically unstable precancerous cells. When cell cycle checkpoints are inactivated, the carcinogenic process can be provoked and has been reported in several human cancers, including hepatocellular carcinoma.[22–24]

There have been increasing studies of the preneoplasia-carcinoma sequence of hepatocellular carcinoma at the molecular level. However, a systemic assessment of telomere length, chromosomal instability, and inactivation of cell cycle checkpoints has not been investigated in defined lesions of human multistep hepatocarcinogenesis. We therefore studied telomere length, micronuclei, and $p21^{WAF1/CIP1}$ expression and their relationship in cirrhotic livers, dysplastic nodules, and hepatocellular carcinomas of hepatitis B virus-associated human multistep hepatocarcinogenesis.

Materials and methods

Tissue Samples and Pathological Examination

We studied hepatitis B virus-associated multistep hepatocarcinogenesis in 24 patients. In total, 19 men and 5 women were enrolled in this study, and their ages ranged from 32 to 60 years (51 ± 7.5 years, mean ± s.d.). They were all positive for serum HBsAg and negative for anti-HCV. There were 30 cirrhotic nodules including six large regenerative nodules, 35 low-grade dysplastic nodules, 15 high-grade dysplastic nodules, 7 dysplastic nodules with hepatocellular carcinoma foci, and 18 hepatocellular carcinomas. Fresh liver tissues, sampled from resected or explanted liver specimens, were snap-frozen in liquid nitrogen and stored at $-70^{\circ}C$ until use. Representative sections were submitted for routine histological examination. Clinical and pathological features of patients are summarized in Table 1. All nodular lesions were evaluated according to the criteria proposed by the International Working Party on the terminology of nodular hepatocellular lesions (Figure 1).[2] Hepatocellular carcinoma differentiation was determined on the basis of the Edmondson and Steiner classification.[25]

Table 1 Clinical and pathological findings of patients

Case no.	*Age*	*Sex*	*Etiology*	*Pathological diagnosis*[a]
1	44	F	HBV	LGDN, HGDN, DN with HCC foci, HCC (2)
2	52	M	HBV	LGDN, HGDN, DN with HCC foci, HCC (2)
3	50	M	HBV	LGDN, HCC (2)
4	60	F	HBV	HGDN, HCC (1)
5	49	M	HBV	LGDN, HCC (2)
6	59	M	HBV	LGDN, HGDN, DN with HCC foci
7	48	M	HBV	LGDN, DN with HCC foci
8	60	M	HBV	HGDN, DN with HCC foci
9	55	F	HBV	LGDN, HGDN
10	54	M	HBV	LGDN, HGDN
11	51	M	HBV	LGDN
12	48	M	HBV	LGDN
13	56	M	HBV	HCC (3)
14	41	M	HBV	HCC (3)
15	43	M	HBV	HCC (3)
16	60	M	HBV	HCC (2)
17	40	M	HBV	HCC (2)
18	54	F	HBV	HCC (2)
19	59	M	HBV	HCC (2)
20	47	M	HBV	HCC (1)
21	45	M	HBV	DN with HCC foci
22	60	M	HBV	HGDN
23	32	F	HBV	LGDN
24	48	M	HBV	LGDN

M: male, F: female, HBV: hepatitis B virus, LGDN: low-grade dysplastic nodule, HGDN: high-grade dysplastic nodule, DN with HCC foci: dysplastic nodule with hepatocellular carcinoma foci, HCC: hepatocellular carcinoma.
[a]HCC grading according to the Edmondson and Steiner classification is in parentheses.

All of the non-hepatocellular carcinoma liver samples showed hepatitis B virus-associated cirrhosis. For comparison with normal livers, non-neoplastic liver samples were obtained from eight patients with metastatic colorectal carcinomas. The controls did not have the hepatitis virus and showed relatively normal liver histology, with the exception of mild steatosis. There were four men and two women, and their ages ranged from 42 to 66 years (54 ± 9.7 years, mean ± s.d.). This study was approved by the Institutional Review Board of Severance Hospital, Yonsei University College of Medicine, and liver specimens were provided by the Liver Cancer Specimen Bank of the National Research Resource Bank Program of the Korea Science and Engineering Foundation of the Ministry of Science and Technology.

Micronuclei Study

Micronuclei of hepatocytes were identified by Feulgen-fast green dyeing technique. Formalin-fixed paraffin-embedded tissue sections (4 μm) were deparaffinized with xylene for 30 min, rehydrated with graded alcohol, and then immersed in 0.1 M hydrochloric acid at 60°C for 5 min. Slides were then immersed in Schiff reagent for 30 min until the nuclei were stained, and were then transferred directly to bisulfate water, followed by rinsing under running tap water. Counterstaining was carried out with 0.1% fast green for 30 s.

The presence of micronuclei was defined using the following criteria: (1) a diameter smaller than one-third of the nucleus, (2) non-refractive to be distinguished from artifacts such as small staining particles, (3) no connection to the main nucleus, and (4) the same staining intensity as the main nucleus, although staining may occasionally be more intense.[19] Hepatocytes with pyknotic nuclei and those that overlapped were not assessed for micronuclei count. The micronuclei index was defined as the number of micronuclei per 3000 hepatocytes. Micronuclei were actually counted in randomly selected fields and at least 3000 hepatocytes were evaluated, which represented about 30, 10–20 and 5% of the areas of cirrhotic nodules, dysplastic nodules, and hepatocellular carcinomas on the basis of 1 cm sized lesion, respectively.

Telomere Terminal Restriction Fragment Length Analysis

Genomic DNA was prepared from 10 to 50 mg of frozen liver tissue using a standard phenol/chloroform extraction after proteinase K treatment. Telomere length was measured by Southern blotting. In total, 2 μg of DNA digested with 100 U of *H*inf I overnight at 37°C was fractionated on a 0.7% agarose gel. Hybridization was carried out with a

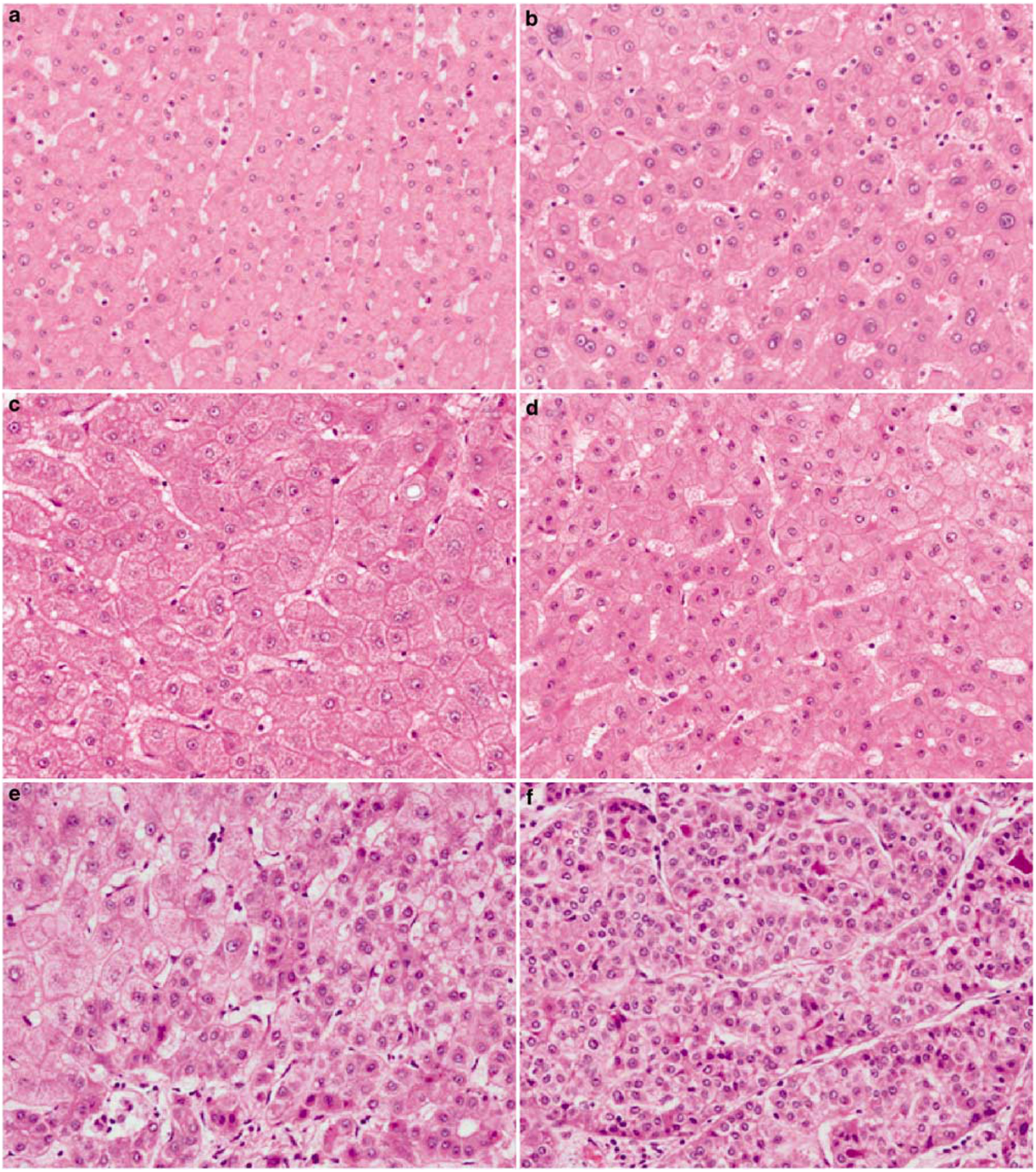

Figure 1 Histological features of normal liver (**a**), cirrhosis (**b**), low-grade dysplastic nodule (**c**), high-grade dysplastic nodule (**d**), dysplastic nodule with hepatocellular carcinoma foci (**e**), and hepatocellular carcinoma (**f**) (H&E stain).

3′-end DIG-labeled d(TTAGGG)$_4$ (Roche Molecular Biochemicals, Mannheim, Germany) at 37°C overnight. After washing the membranes, hybridizations were detected as recommended by the manufacturer (Roche Molecular Biochemicals). The mean telomere terminal restriction fragment lengths were calculated as described earlier.[26] Briefly, the resulting X-ray film was scanned with a luminescent image analyzer (Fujifilm, Tokyo, Japan), and the telomere signal in each lane quantified in a grid object, defined as a single column with 25 rows, using the Image Gauge Software 2.54 (Fujifilm).

Immunohistochemical Analysis of $p21^{WAF1/CIP1}$

Paraffin sections were deparaffinized in xylene for 30 min, and then rehydrated with graded alcohol. Endogenous peroxidase activity was quenched in a 3% hydrogen peroxide/methanol solution for 10 min. For antigen retrieval, sections were boiled in 100 mM sodium citrate, pH 6.0, for 15 min in a microwave oven. A monoclonal primary antibody of $p21^{WAF1/CIP1}$ (Clone SX118, DAKO, Glostrup, Denmark) at a 1:50 dilution was applied for 30 min at room temperature, and then incubated overnight at 4°C. After washing in PBS, incubation with the secondary antibody was carried out using the DAKO EnVision Rabbit/Mouse kit for 30 min at room temperature, after which sections were developed with diaminobenzidine (DAKO). The sections were then counterstained with hematoxylin, dehydrated using graded alcohol, and cleared in xylene.

For interpretation of the immunohistochemical stain results, hepatocytes were counted in at least five random high-power fields ($\times 400$ magnification) so that the number of hepatocytes scored was at least 500 in every case. Dark brown nuclear staining of hepatocytes was scored as positive for $p21^{WAF1/CIP1}$ and detected in representative fields of each nodular lesion. Results were expressed as the $p21^{WAF1/CIP1}$ labeling index, which is defined as the percentage of positive hepatocytes.

Statistical Analysis

Statistical analysis was carried out using SPSS software (SPSS, Inc., Chicago, IL, USA). Mann–Whitney test was applied to compare telomere terminal restriction fragment length, micronuclei index, and $p21^{WAF1/CIP1}$ labeling index between each group. Correlation was estimated using Pearson's correlation coefficient. Significance was set at $P<0.05$ for all tests.

Results

Gradual Increase of Micronuclei Index and Telomere Shortening during Hepatitis B Virus-Related Multistep Hepatocarcinogenesis

Micronuclei formation was investigated in each hepatic nodular lesion and background liver with cirrhosis (Figure 2). Normal liver samples showed no micronuclei. The majority of cirrhosis cases (27 cases, 90%) showed no micronuclei and three cases (10%) showed one micronucleus per 3000 hepatocytes. In low-grade dysplastic nodules, there were 12 cases (34%) without micronuclei, 17 (49%) with one micronucleus, and six (17%) with more than one micronucleus per 3000 hepatocytes. Micronuclei >1 per 3000 hepatocytes were found in 13 (87%) of the high-grade dysplastic nodules and in all the cases (100%) of dysplastic nodules with hepatocellular carcinoma foci and hepatocellular carcinomas. The micronuclei index (number of micronuclei per 3000 hepatocytes) gradually increased along with the progression of hepatocarcinogenesis and it was 0.1 ± 0.06 (mean ± s.d.) (range, 0–1) in cirrhosis, 0.9 ± 0.16 (0–4) in low-grade dysplastic nodules, 3.1 ± 0.38 (0–5) in high-grade dysplastic nodules, 4.0 ± 0.58 (2–6) in dysplastic nodules with hepatocellular carcinoma foci, and 12.2 ± 1.93 (4–30) in hepatocellular carcinomas (Figure 3). A significant increase in the micronuclei index occurred between cirrhosis and low-grade dysplastic nodules ($P<0.001$), as well as between low-grade dysplastic nodules and high-grade dysplastic nodules ($P<0.001$). Hepatocellular carcinomas showed the highest micronuclei index, which was significantly higher compared with that of high-grade dysplastic nodules and dysplastic nodules with hepatocellular carcinoma foci ($P=0.002$).

Terminal restriction fragment length was measured by Southern blot analysis and representative cases are shown in Figure 4. Terminal restriction fragment length gradually decreased according to the progression of multistep hepatocarcinogenesis. Telomere length (kb) was 8.1 ± 0.31 (mean ± s.d.) (range, 7.3–9.3) in normal livers, 7.6 ± 0.29 (4.1–11.3) in cirrhotic livers, 7.2 ± 0.30 (3.6–10.4) in low-grade dysplastic nodules, 6.6 ± 0.68 (2.9–11.5) in high-grade dysplastic nodules, 6.2 ± 0.68 (3.6–8.7) in dysplastic nodules with hepatocellular carcinoma foci, and 6.6 ± 0.57 (3.4–12.0) in hepatocellular carcinomas (part of the telomere data was from an earlier study).[12] A significant reduction in telomere length was found in high-grade dysplastic nodules and dysplastic nodules with hepatocellular carcinoma ($P=0.024$) and hepatocellular carcinomas ($P=0.031$) compared with normal and cirrhotic livers (Figure 5). However, differences between cirrhotic livers and low-grade dysplastic nodules, low-grade dysplastic nodules and high-grade dysplastic nodules, high-grade dysplastic nodules and dysplastic nodules with hepatocellular carcinoma foci, and dysplastic nodules with hepatocellular carcinoma foci and hepatocellular carcinomas failed to reach statistical significance.

The micronuclei index showed a significant correlation with telomere shortening ($r=-0.227$, $P=0.016$); hepatic nodules with a higher micronuclei index showed shorter telomere length (Figure 6a). Among 35 low-grade dysplastic nodules, 23 cases (66%) showed micronuclei formation and their telomere length was 6.3 ± 1.32 kb (range, 3.6–9.3), whereas it was 8.9 ± 1.18 kb (range, 6.9–10.4) in low-grade dysplastic nodules without micronuclei. Telomeres were significantly shorter in low-grade dysplastic nodules with micronuclei than in those without ($P<0.001$) (Figure 6b). It is interesting that four cases (11%) of low-grade dysplastic nodules and five cases (33%) of high-grade dysplastic nodules showed short telomere <5 kb and all of them showed micronuclei formation.

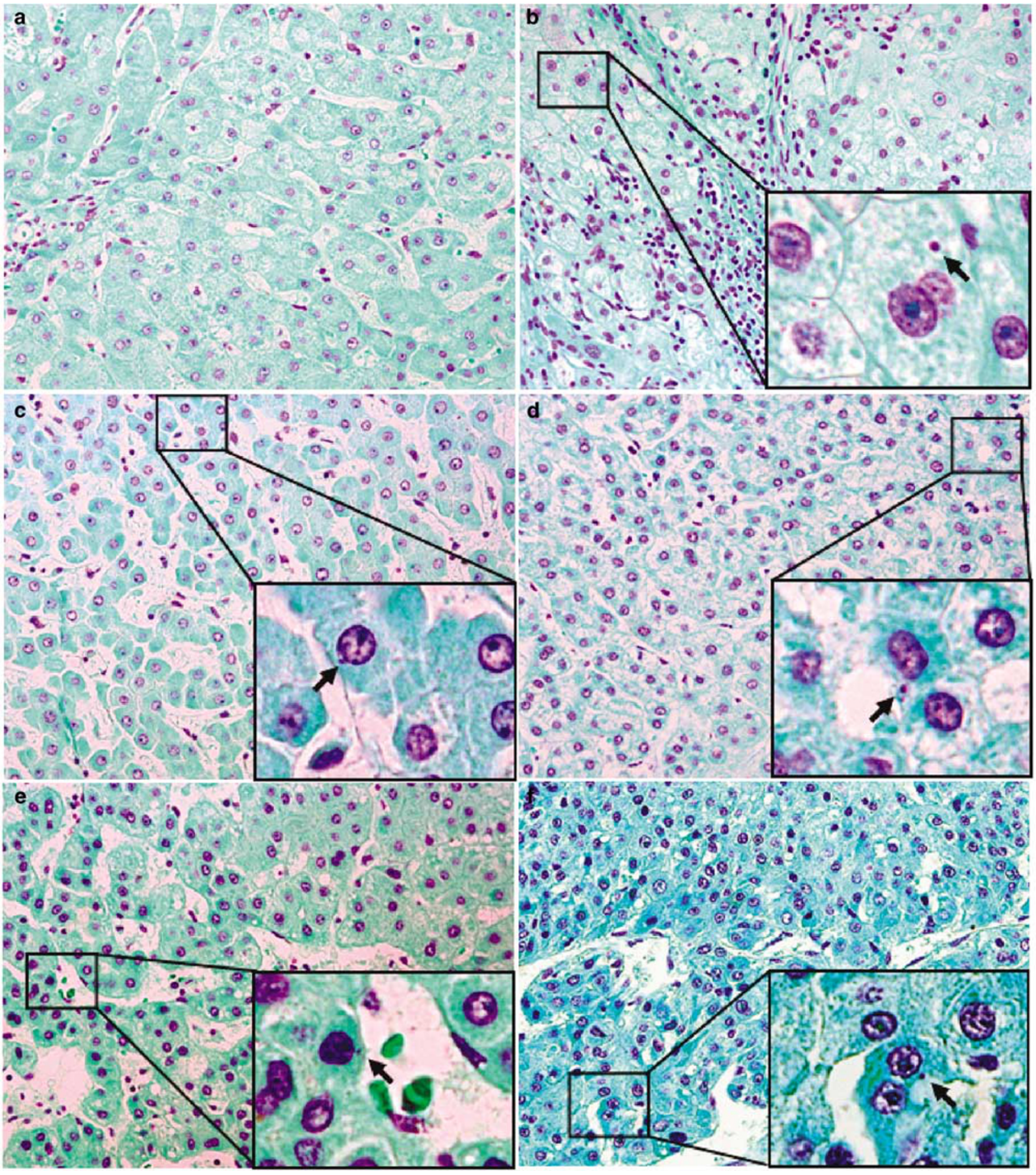

Figure 2 Micronuclei during hepatitis B virus-associated multistep hepatocarcinogenesis. Representative photographs of micronuclei detected in normal liver (**a**), cirrhosis (**b**), low-grade dysplastic nodule (**c**), high-grade dysplastic nodule (**d**), dysplastic nodule with hepatocellular carcinoma foci (**e**), and hepatocellular carcinoma (**f**). No micronuclei were found in normal liver. Hepatocytes with micronuclei are marked by a square line and higher power features are presented in the inset of lower right corner (Feulgen-fast green stain).

Expression of p21$^{WAF1/CIP1}$ during Hepatitis B Virus-Related Multistep Hepatocarcinogenesis

p21$^{WAF1/CIP1}$, cell cycle checkpoint function was analyzed by immunohistochemical staining in each hepatic nodule and hepatocellular carcinoma (Figure 7). The p21$^{WAF1/CIP1}$ labeling index was 9.0 ± 5.42 (mean $\pm$ s.d.) (range, 3.1–18.6) in normal livers, 20.0 ± 13.33 (1.6–47.2) in cirrhotic livers, 8.3 ± 6.24 (2.1–33.7) in low-grade dysplastic

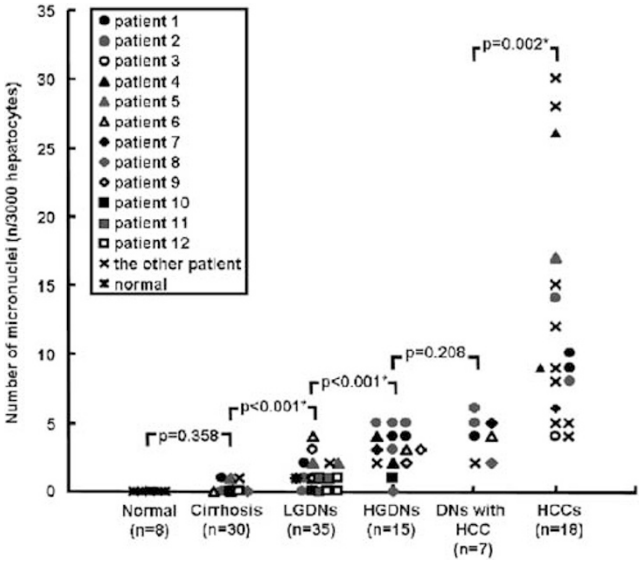

Figure 3 Comparison of micronuclei index in normal livers, cirrhotic livers, low-grade dysplastic nodules (LGDNs), high-grade dysplastic nodules (HGDNs), dysplastic nodules with hepatocellular carcinoma foci (DN with HCC), and hepatocellular carcinomas (HCCs). The patients (number 1–12) who had multiple lesions including hepatocellular carcinoma and dysplastic nodules are each characterized by different symbols, and the other patients who had hepatocellular carcinoma without synchronously developed dysplastic nodules marked by the same symbol (x). *Statistical significance ($P<0.05$).

nodules, 9.3 ± 10.74 (0.8–44.7) in high-grade dysplastic nodules, 11.9 ± 8.23 (5.7–29.7) in dysplastic nodules with hepatocellular carcinoma foci, and 11.7 ± 20.38 (0.4–85.4) in hepatocellular carcinomas. The $p21^{WAF1/CIP1}$ labeling index in cirrhotic livers was significantly higher than that of normal livers ($P=0.024$). It was markedly decreased in low-grade dysplastic nodules, high-grade dysplastic nodules, and hepatocellular carcinomas compared with cirrhotic livers ($P<0.05$) (Figure 8). Differences between low-grade dysplastic nodules and high-grade dysplastic nodules, high-grade dysplastic nodules and hepatocellular carcinomas, and high-grade dysplastic nodules with hepatocellular carcinoma foci and hepatocellular carcinomas failed to reach statistical significance.

Telomere length showed a significant correlation with $p21^{WAF1/CIP1}$ labeling index ($r=0.378$, $P<0.001$); hepatic nodules with shorter telomeres showed lower $p21^{WAF1/CIP1}$ labeling index (Figure 9). However, $p21^{WAF1/CIP1}$ labeling index did not show a significant correlation with the micronuclei index ($P>0.05$), nor did it differ significantly between low-grade dysplastic nodules with or without micronuclei formation. It is interesting to note that $p21^{WAF1/CIP1}$ labeling index was 6.0 ± 2.20 (mean ± s.d.) (range, 3.9–9.1) in low-grade dysplastic nodules with short telomere <5 kb and 2.7 ± 1.42 (0.8–4.4) in high-grade dysplastic nodules with short telomere <5 kb and their expression of $p21^{WAF1/CIP1}$ checkpoint was inactivated.

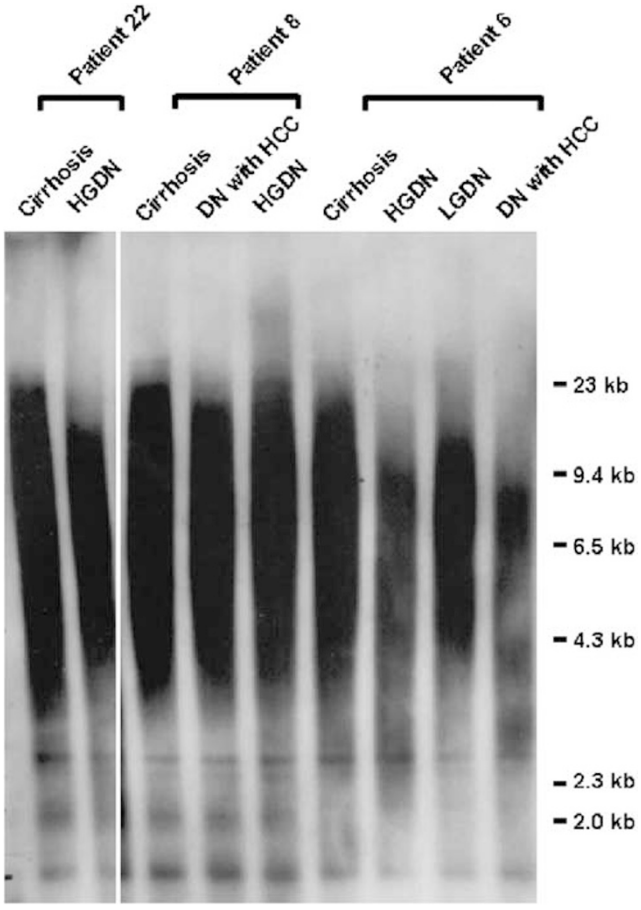

Figure 4 Telomere terminal restriction fragment length during hepatitis B virus-associated multistep hepatocarcinogenesis. Southern blot analysis of terminal restriction fragment length in cirrhosis, low-grade dysplastic nodule (LGDN), high-grade dysplastic nodule (HGDN), and dysplastic nodule with hepatocellular carcinoma foci (DNs with HCC).

Discussion

There has been increasing evidence of a multistep process in human hepatocarcinogenesis. Allelic alterations have been reported in early stages of hepatocarcinogensis, however, the detailed molecular mechanism underlying the preneoplasia-carcinoma sequence during hepatocarcinogenesis is poorly understood.[27–30]

Chromosomal instability is a characteristic of hepatitis B virus-related hepatocarcinogenesis.[11] The telomere, stabilizing the chromosome ends by end-to-end fusion, is shortened with each cell division of somatic cells, as it is not replicated during the S phase of the cell cycle, and loss of the telomere leads to the formation of chromosomal instability.[7,8] In this study, telomere length showed a gradual shortening during hepatitis B virus-related multistep hepatocarcinogenesis, which was consistent with earlier reports.[12,13] The micronucleus, an indicator of chromosomal instability, was reported to be associated with an increase in chromosomal

alteration in an *in vitro* and *in vivo* study.[14–18] The studies revealed that the frequency of micronuclei gradually increased during human multistep hepatocarcinogenesis. Micronuclei >1 per 3000 hepatocytes was found in 17% of low-grade dysplastic nodules, 87% of high-grade dysplastic nodules, and 100% of dysplastic nodules with hepatocellular carcinoma foci and hepatocellular carcinomas in contrast to all normal livers and 90% of cirrhotic livers showed no micronuclei. The micronuclei index (number of micronulei per 3000 hepatocytes) also increased according to the progression of multistep hepatocarcinogenesis. A significant increase was found between cirrhotic livers and low-grade dysplastic nodules, low-grade dysplastic nodules and high-grade dysplastic nodules, and dysplastic nodules with hepatocellular carcinoma foci and hepatocellular carcinomas and hepatocellular carcinomas showed the highest levels of micronuclei. The micronuclei index was negatively correlated with telomere length; hepatic nodules with short telomeres had high numbers of micronuclei. Taken together, these results show that telomere shortening and chromosomal instability start to occur in low-grade dysplastic nodules and high-grade dysplastic nodules, an early stage of hepatocarcinogenesis.

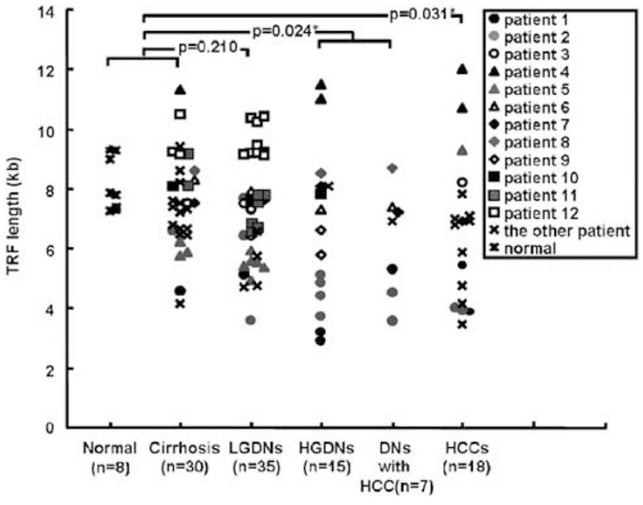

Figure 5 Comparison of telomere terminal restriction fragment (TRF) length (kb) in normal livers, cirrhotic livers, low-grade dysplastic nodules (LGDNs), high-grade dysplastic nodules (HGDNs), dysplastic nodules with hepatocellular carcinoma foci (DNs with HCC), and hepatocellular carcinomas (HCCs). The patients (number 1–12) who had multiple lesions including hepatocellular carcinoma and dysplastic nodules are each characterized by different symbols, and the other patients who had hepatocellular carcinoma without synchronously developed dysplastic nodules marked by the same symbol (x). *Statistical significance ($P<0.05$).

Inactivation of the DNA damage checkpoint has recently been suggested as a critical feature in carcinogenesis models.[22,23] In this study, $p21^{WAF1/CIP1}$ expression was significantly higher in cirrhotic livers than in normal livers, and these data indicate that preservation of the $p21^{WAF1/CIP1}$ checkpoint is an important defense mechanism in cirrhosis, which is a risk factor for the development of hepatocellular carcinoma, in which chromosomal instability and telomere shortening start to occur, although at a very low level. In contrast, $p21^{WAF1/CIP1}$ expression significantly decreased in both low-grade dysplastic nodules and high-grade dysplastic nodules compared with cirrhosis, and it was also significantly depressed in hepatocellular carcinomas compared with cirrhosis. The $p21^{WAF1/CIP1}$ labeling index showed a significant positive correlation with telomere length ($P<0.001$), and hepatic nodules with shorter telomeres had lower $p21^{WAF1/CIP1}$ labeling index. Therefore, cooperation between telomere shortening, chromosomal instability, and loss of the

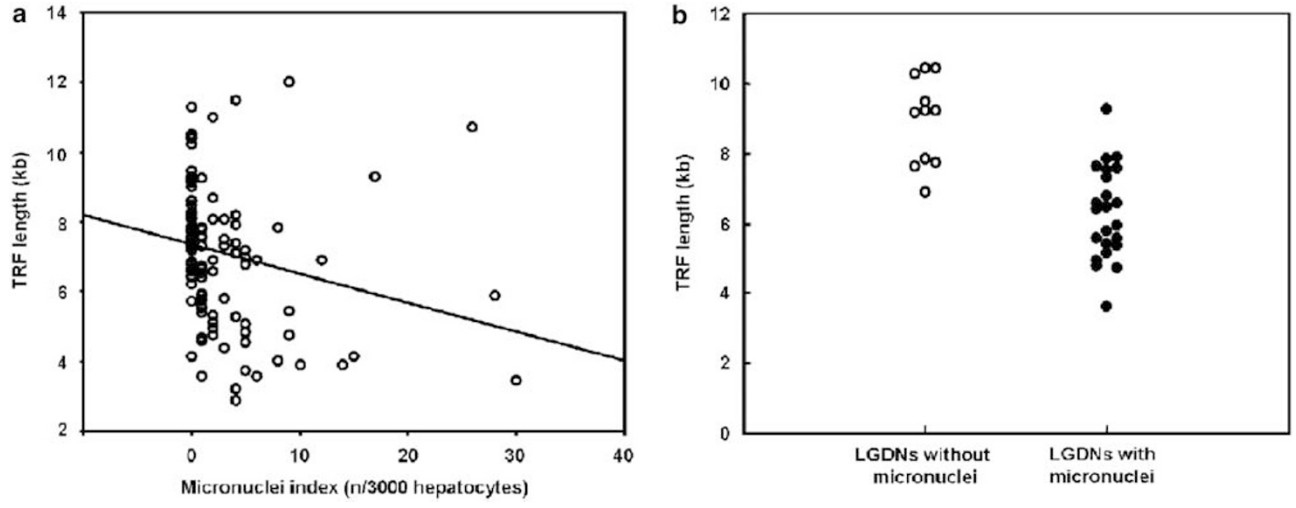

Figure 6 Relationship between micronuclei and telomere terminal restriction fragment (TRF) length. (**a**) The number of micronuclei showing a significant negative correlation with telomere length ($r=-0.227$, $P=0.016$). (**b**) Comparison of terminal restriction fragment length between low-grade dysplastic nodules (LGDNs) with and without micronuclei. Low-grade dysplastic nodules with micronuclei have significantly shorter telomeres than those without ($P<0.001$).

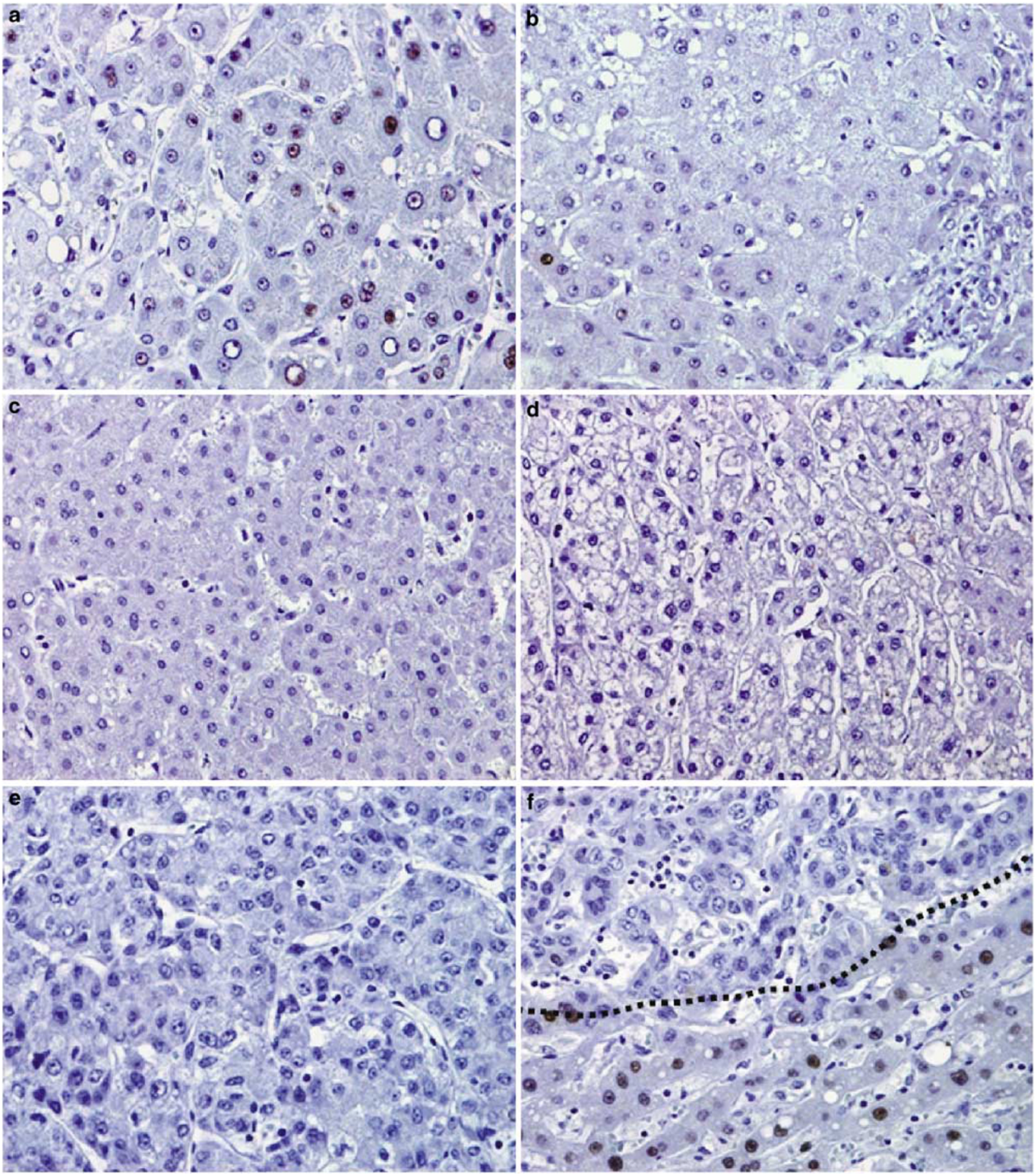

Figure 7 Expression of $p21^{WAF1/CIP1}$ during hepatitis B virus-associated multistep hepatocarcinogenesis. Representative photographs of $p21^{WAF1/CIP1}$ immunostaining in cirrhotic liver (**a**), low-grade dysplastic nodule (**b**), high-grade dysplastic nodule (**c**), dysplastic nodule with hepatocellular carcinoma foci (**d**), and hepatocellular carcinoma (**e** and **f**). The border of hepatocellular carcinoma is marked by a dotted line (**f**). Note that cirrhosis (below the line) shows higher $p21^{WAF1/CIP1}$ expression compared with hepatocellular carcinoma (above the line).

$p21^{WAF1/CIP1}$ checkpoint might evoke further progression during multistep hepatocarcinogenesis.

The natural outcome of low-grade dysplastic nodules has been controversial, whereas high-grade dysplastic nodules were shown to be closely associated with an increased risk of malignant transformation.[4–6] Kobayashi *et al*[6] reported that cumulative hepatocellular carcinoma development rates at the first and fifth years were 46.2 and 80.8% for high-grade dysplastic nodules, 2.6 and 36.6% for

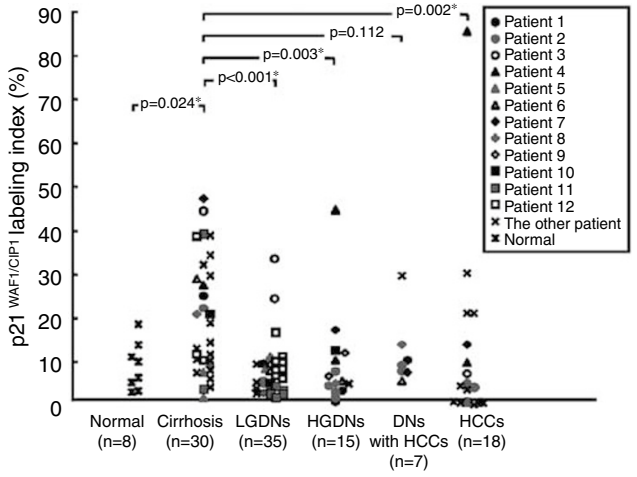

Figure 8 Comparison of p21$^{WAF1/CIP1}$ labeling index in normal livers, cirrhotic livers, low-grade dysplastic nodules (LGDNs), high-grade dysplastic nodules (HGDNs), dysplastic nodules with hepatocellular carcinoma foci (DNs with HCC), and hepatocellular carcinomas (HCCs). The patients (number 1–12) who had multiple lesions including hepatocellular carcinoma and dysplastic nodules are each characterized by different symbols, and the other patients who had hepatocellular carcinoma without synchronously developed dysplastic nodules marked by the same symbol (x). *Statistical significance ($P<0.05$).

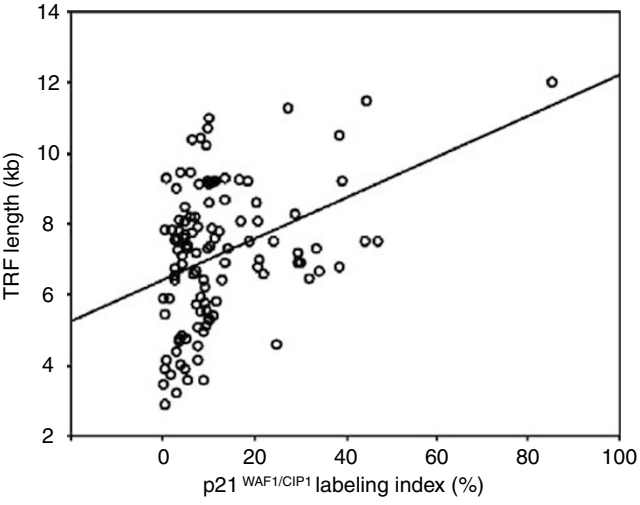

Figure 9 Relationship between p21$^{WAF1/CIP1}$ labeling index and telomere terminal restriction fragment (TRF) length. The p21$^{WAF1/CIP1}$ labeling index shows a significant positive correlation with terminal restriction fragment length ($r=0.378$, $P<0.001$).

low-grade dysplastic nodules, and 3.3 and 12.4% for cirrhotic regenerative nodules, respectively. Borzio *et al*[5] reported that high-grade dysplastic nodules were strong predictors of malignant transformation; however, low-grade dysplastic nodules were not at increased risk for hepatocellular carcinoma. Interestingly, this study found that 11% of low-grade dysplastic nodules showed short telomere (<5 kb) and all of them had micronuclei formation. Cells with critically shortened telomeres gain further chromosomal instability through breakage-fusion-bridge cycles during replication, which has a catastrophic effect on cells. However, telomerase reactivation can stabilize the chromosome ends and produce aberrant yet stable chromosomes; these cells then gain immortality.[31] We earlier reported that the reactivation of telomerase occurred in dysplastic nodules, an early stage of hepatocarcinogenesis, and moreover, 7% of low-grade dysplastic nodules showed telomerase activation in our earlier study, although the majority of low-grade dysplastic nodules were telomerase negative.[12,32] In this study, expression of the p21$^{WAF1/CIP1}$ checkpoint was significantly depressed in low-grade dysplastic nodules compared with cirrhosis, and all of the low-grade dysplastic nodules with short telomere (<5 kb) showed inactivation of p21$^{WAF1/CIP1}$ checkpoint. Taken together, it suggests that low-grade dysplastic nodules might be a biologically heterogeneous group, although histological differences are very hard to detect. A small fraction, about 11% of low-grade dysplastic nodules with telomere shortening, micronuclei, and inactivation of the p21$^{WAF1/CIP1}$ checkpoint, might have the potential to progress to further, more advanced lesions in human hepatocarcinogenesis.

In conclusion, chromosomal instability, telomere shortening, and inactivation of the p21$^{WAF1/CIP1}$ checkpoint occur in both low-grade dysplastic nodules and high-grade dysplastic nodules, which are preneoplastic lesions of human multistep hepatocarcinogenesis. Their co-occurrence is suggested to be critical for malignant transformation during hepatitis B virus-associated human multistep hepatocarcinogenesis.

Acknowledgements

This work was supported by a Korea Science and Engineering Foundation (KOSEF) grant funded by the Korean Ministry of Science and Technology (MOST) (R13-2002-054-03004-0) and FG06-11-04 from the 21C Frontier Functional Human Genome Project (MOST), a faculty research grant from Yonsei University College of Medicine for 2007 (6-2007-0093).

References

1 Parkin DM, Bray F, Ferlay J, *et al.* Estimating the world cancer burden: Globocan 2000. Int J Cancer 2001;94:153–156.
2 Terminology of nodular hepatocellular lesions. International Working Party. Hepatology 1995;22:983–993.
3 Theise ND, Park YN, Kojiro M. Dysplastic nodules and hepatocarcinogenesis. Clin Liver Dis 2002;6:497–512.
4 Hytiroglou P, Park YN, Krinsky G, *et al.* Hepatic precancerous lesions and small hepatocellular carcinoma. Gastroenterol Clin North Am 2007;36: 867–887, vii.

5 Borzio M, Fargion S, Borzio F, *et al.* Impact of large regenerative, low grade and high grade dysplastic nodules in hepatocellular carcinoma development. J Hepatol 2003;39:208–214.
6 Kobayashi M, Ikeda K, Hosaka T, *et al.* Dysplastic nodules frequently develop into hepatocellular carcinoma in patients with chronic viral hepatitis and cirrhosis. Cancer 2006;106:636–647.
7 Ishikawa F. Telomere crisis, the driving force in cancer cell evolution. Biochem Biophys Res Commun 1997;230:1–6.
8 Murnane JP. Telomeres and chromosome instability. DNA Repair 2006;5:1082–1092.
9 Wilkens L, Flemming P, Gebel M, *et al.* Induction of aneuploidy by increasing chromosomal instability during dedifferentiation of hepatocellular carcinoma. Proc Natl Acad Sci USA 2004;101:1309–1314.
10 Nishida N, Nishimura T, Ito T, *et al.* Chromosomal instability and human hepatocarcinogenesis. Histol Histopathol 2003;18:897–909.
11 Boyault S, Rickman DS, de Reynies A, *et al.* Transcriptome classification of HCC is related to gene alterations and to new therapeutic targets. Hepatology 2007;45:42–52.
12 Oh BK, Jo Chae K, Park C, *et al.* Telomere shortening and telomerase reactivation in dysplastic nodules of human hepatocarcinogenesis. J Hepatol 2003;39: 786–792.
13 Oh BK, Kim YJ, Park C, *et al.* Up-regulation of telomere-binding proteins, TRF1, TRF2, and TIN2 is related to telomere shortening during human multistep hepatocarcinogenesis. Am J Pathol 2005;166:73–80.
14 Countryman PI, Heddle JA. The production of micronuclei from chromosome aberrations in irradiated cultures of human lymphocytes. Mutat Res 1976;41:321–332.
15 Fenech M, Holland N, Chang WP, *et al.* The HUman MicroNucleus Project—an international collaborative study on the use of the micronucleus technique for measuring DNA damage in humans. Mutat Res 1999;428:271–283.
16 Livezey KW, Negorev D, Simon D. Increased chromosomal alterations and micronuclei formation in human hepatoma HepG2 cells transfected with the hepatitis B virus HBX gene. Mutat Res 2002;505:63–74.
17 Cliet I, Fournier E, Melcion C, *et al. In vivo* micronucleus test using mouse hepatocytes. Mutat Res 1989;216:321–326.
18 Van Goethem F, Ghahroudi MA, Castelain P, *et al.* Frequency and DNA content of micronuclei in rat parenchymal liver cells during experimental hepatocarcinogenesis. Carcinogenesis 1993;14:2397–2406.
19 de Almeida TM, Leitao RC, Andrade JD, *et al.* Detection of micronuclei formation and nuclear anomalies in regenerative nodules of human cirrhotic livers and relationship to hepatocellular carcinoma. Cancer Genet Cytogenet 2004;150:16–21.
20 d'Adda di Fagagna F, Reaper PM, Clay-Farrace L, *et al.* A DNA damage checkpoint response in telomere-initiated senescence. Nature 2003;426:194–198.
21 Brown JP, Wei W, Sedivy JM. Bypass of senescence after disruption of p21CIP1/WAF1 gene in normal diploid human fibroblasts. Science 1997;277: 831–834.
22 Bartkova J, Horejsi Z, Koed K, *et al.* DNA damage response as a candidate anti-cancer barrier in early human tumorigenesis. Nature 2005;434:864–870.
23 Michaloglou C, Vredeveld LC, Soengas MS, *et al.* BRAFE600-associated senescence-like cell cycle arrest of human naevi. Nature 2005;436:720–724.
24 Plentz RR, Park YN, Lechel A, *et al.* Telomere shortening and inactivation of cell cycle checkpoints characterize human hepatocarcinogenesis. Hepatology 2007;45:968–976.
25 Edmondson HA, Steiner PE. Primary carcinoma of the liver: a study of 100 cases among 48,900 necropsies. Cancer 1954;7:462–503.
26 Kruk PA, Rampino NJ, Bohr VA. DNA damage and repair in telomeres: relation to aging. Proc Natl Acad Sci USA 1995;92:258–262.
27 Maggioni M, Coggi G, Cassani B, *et al.* Molecular changes in hepatocellular dysplastic nodules on microdissected liver biopsies. Hepatology 2000;32: 942–946.
28 Sun M, Eshleman JR, Ferrell LD, *et al.* An early lesion in hepatic carcinogenesis: loss of heterozygosity in human cirrhotic livers and dysplastic nodules at the 1p36-p34 region. Hepatology 2001;33:1415–1424.
29 Tornillo L, Carafa V, Sauter G, *et al.* Chromosomal alterations in hepatocellular nodules by comparative genomic hybridization: high-grade dysplastic nodules represent early stages of hepatocellular carcinoma. Lab Invest 2002;82:547–553.
30 Lee JM, Wong CM, Ng IO. Hepatitis B virus-associated multistep hepatocarcinogenesis: a stepwise increase in allelic alterations. Cancer Res 2008;68: 5988–5996.
31 Hackett JA, Greider CW. Balancing instability: dual roles for telomerase and telomere dysfunction in tumorigenesis. Oncogene 2002;21:619–626.
32 Oh BK, Kim YJ, Park YN, *et al.* Quantitative assessment of hTERT mRNA expression in dysplastic nodules of HBV-related hepatocarcinogenesis. Am J Gastroenterol 2006;101:831–838.